Iowa State University
Digital Repository

Proceedings of the ARPA/AFML Review of Quantitative NDE, June 1974–July 1975

Interdisciplinary Program for Quantitative Flaw Definition Annual Reports

7-1975

# Adaptive Learning Network Approach to Defect Characterization

Anthony N. Mucciardi
*Adaptronics, Inc.*

Follow this and additional works at: http://lib.dr.iastate.edu/cnde_yellowjackets_1975

Part of the Materials Science and Engineering Commons, and the Structures and Materials Commons

## Recommended Citation

Mucciardi, Anthony N., "Adaptive Learning Network Approach to Defect Characterization" (1975). *Proceedings of the ARPA/AFML Review of Quantitative NDE, June 1974–July 1975*. 7.
http://lib.dr.iastate.edu/cnde_yellowjackets_1975/7

This 5. Signal Processing is brought to you for free and open access by the Interdisciplinary Program for Quantitative Flaw Definition Annual Reports at Iowa State University Digital Repository. It has been accepted for inclusion in Proceedings of the ARPA/AFML Review of Quantitative NDE, June 1974–July 1975 by an authorized administrator of Iowa State University Digital Repository. For more information, please contact digirep@iastate.edu.

# Adaptive Learning Network Approach to Defect Characterization

**Abstract**
The overall objective of this work was to demonstrate feasibility of adaptive nonlinear signal processing techniques applied to characterization of ultrasonic nondestructive testing (UNDT) waveforms for accurate inferences of flat -bottom hole sizes. The classified waveforms were ultrasonic pulse echoes obtained from two different sets of 7075-T6 aluminum area-amplitude test blocks and three different transducers. The eight flat-bottom hole defect sizes ranged from 1/64 to 8/64 inch in steps of l/64 inch.

**Disciplines**
Materials Science and Engineering | Structures and Materials

This 5. signal processing is available at Iowa State University Digital Repository: http://lib.dr.iastate.edu/cnde_yellowjackets_1975/7

# ADAPTIVE LEARNING NETWORK APPROACH TO DEFECT CHARACTERIZATION

Anthony N. Mucciardi
Adaptronics, Inc.
McLean, Virginia

The overall objective of this work was to demonstrate feasibility of adaptive nonlinear signal processing techniques applied to characterization of ultrasonic nondestructive testing (UNDT) waveforms for accurate inferences of flat-bottom hole sizes. The classified waveforms were ultrasonic pulse echoes obtained from two different sets of 7075-T6 aluminum area-amplitude test blocks and three different transducers. The eight flat-bottom hole defect sizes ranged from 1/64 to 8/64 inch in steps of 1/64 inch.

The ultrasonic equipment used in these studies was specially selected to provide as great a bandwidth as possible so that the ultrasonic waveforms would have maximum information content. Ultrasonic pulses were generated and directed into area-amplitude aluminum test blocks. The pulses reflected by circular flat bottom holes were received by the transducer and amplified in the ultrasonic instrumentation. The pulses were recorded in a Biomation 8100 transient recorder.

The Biomation recorder digitized the received signal and stored the digital information in its shift register memory. The pulse information was played back for inspection on an oscilloscope and transmitted to the memory of a Supernova computer for further processing. The model 8100 has a 2,048 word memory, so sampling at 100 MHz permitted storage of 20.48 $\mu$sec of data. This 20.48 window was sufficient to cover the signal of interest on these test blocks (i.e., its pulse reflected from the defect) if the start of the sampling window was delayed by 20 $\mu$sec. A block diagram of the data acquisition system is shown in Fig. 1.

The test specimens containing an artificial defect used in this project were area-amplitude test blocks prepared in accordance with ASTM E127-64. These blocks were fabricated from 7075-T6 aluminum alloy. Each of the test blocks is 3.75 inches long and 2 inches in diameter. Flat-bottomed holes are drilled along the axis of the block from one end to a depth of 3/4 inch. The holes vary in diameter from 1/64 to 8/64 inches in increments of 1/64 inch. A typical block is illustrated in Fig. 2.

Two different sets of test blocks were fabricated by Trienco. The second set, made by Automation Industries, was used to provide an independent set of blocks. In addition to the area-amplitude blocks, a special block was available to use as a reference standard. This block was 3 inches long and contained no holes. The backwall echo was recorded before and after tests made with the other blocks and a comparison of the before and after tests was used to confirm that the operating conditions of the test system had not changed.

A set of equipment was selected for this project as shown in the block diagram of Fig. 1. A Panametrics 5050PR pulser-receiver was used for generating the ultrsonic pulse, which drives the transducer, and for amplifying the

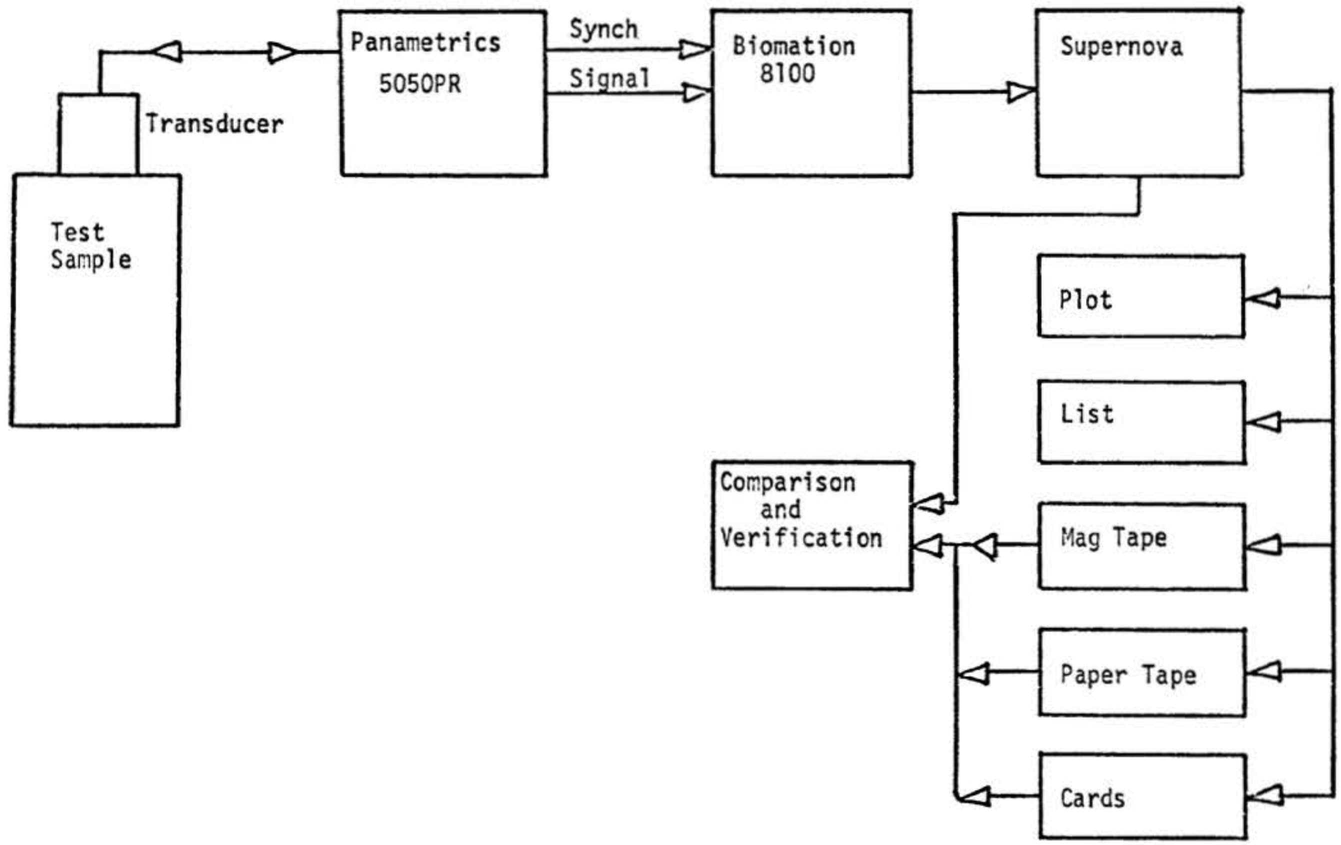


Fig. 1. Block diagram of ultrasonic waveform acquisition system.

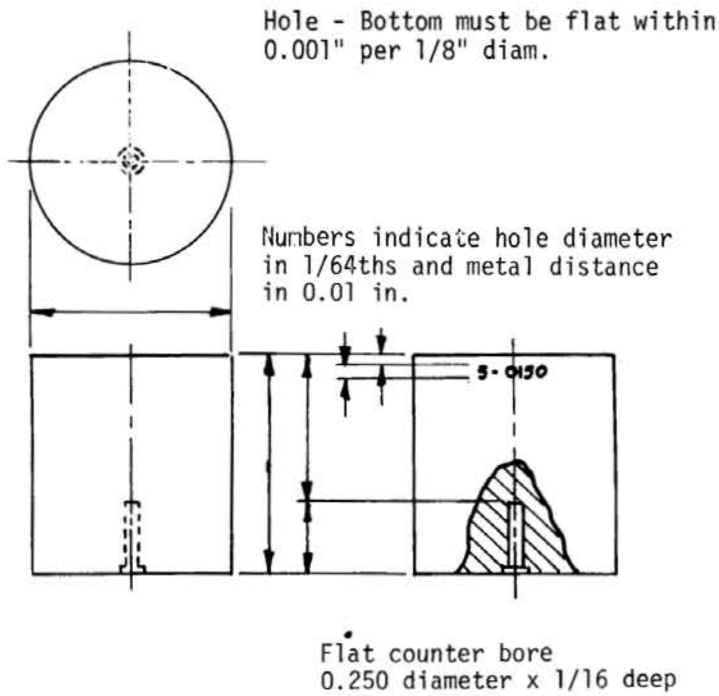


Fig. 2. Typical test block.

reflected pulses detected by the transducer. This instrument was selected because of the exceptionally large bandwidth of the amplifier which extends from approximately 0.5 to 35 MHz. The ultrasonic transducers used were also manufactured by Panametrics. All transducers were nominally 5 MHz. Transducers with diameters of 0.5, 0.75 and 1.0 inch were used for different tests during the project. The spectra produced at the output jack of the 5050PR are shown in Fig. 3a, b, and c for the 0.5, 0.75 and 1.0 inch transducers, respectively. The responses shown in Fig. 3 were obtained by selecting and gating the backwall echo from a 3 inch long test block. Consequently, the spectra are typically measured 6 inches from the transducer and averaged over a diameter equal to that of the transducer. The controls on the 5050PR were set to the same condition normally used with each of the transducers when the spectra were obtained. The frequency range covered by the spectrum analyzer is from 0 to 10 MHz with a dispersion of 1 MHz per major division. The 0.5 inch transducer produces a pulse with appreciable energy in the band from 4 MHz to 7.5 MHz. The 0.75 inch diameter transducer has appreciable energy from approximately 3.8 MHz to 8.6 MHz. The largest transducer, the 1.0 inch diameter transducer, has most of the energy concentrated between 5.5 and 7.2 MHz with the peak occurring at approximately 6.5 MHz. Therefore, these are quite different characteristics for each of these three "5 MHz" transducers and this complicates the data analysis and classification tasks.

A total of 127 test shots were recorded for analysis among the two sets of eight flat-bottom hole samples and three transducers. (The data were recorded by personnel at Babcock & Wilcox, Lynchburg Research Center.) As described above, only a portion of the 20.48 $\mu$sec waveform contains the echo reflected from the hole defect. A plot of the pertinent pulse echo defect data for test 127 is shown in Fig. 4 for illustrative purposes. The time scale is 1.4 $\mu$sec between the 490th and 630th data samples shown.

The data base was divided into three sub-sets as follows. The fitting subset was used to determine the coefficients of the elements in the adaptive learning network (ALN) classifier model (described below). The selection subset was used to select those elements with the most generalizing capability and to prevent overfitting the design data subset. The evaluation subset was used to check the resultant network's ability to predict flat-bottom hole sizes with comparable accuracy for records that had not been used in the modeling procedure. Error rates on this third data subset are the true measure of the generalizing ability of the ALN flat-bottom hole classification model. Data obtained from the 0.5 inch and 0.75 inch transducers from both sets of test blocks were arbitrarily divided among the three data sub-sets such that each subset contained equally representative examples of the UNDT experimental (parameterized) records.

An alternative evaluation subset contained the entire series of eight echoes from the one-inch transducer. Since no member of this series was included in either the fitting or selection subsets (that is, the classifier was never exposed to a one-inch transducer record in its synthesis), the classifier performance on this subset was viewed as a demonstration of the degree of insensitivity of the system to transducers different from those used in the classifier design procedure.

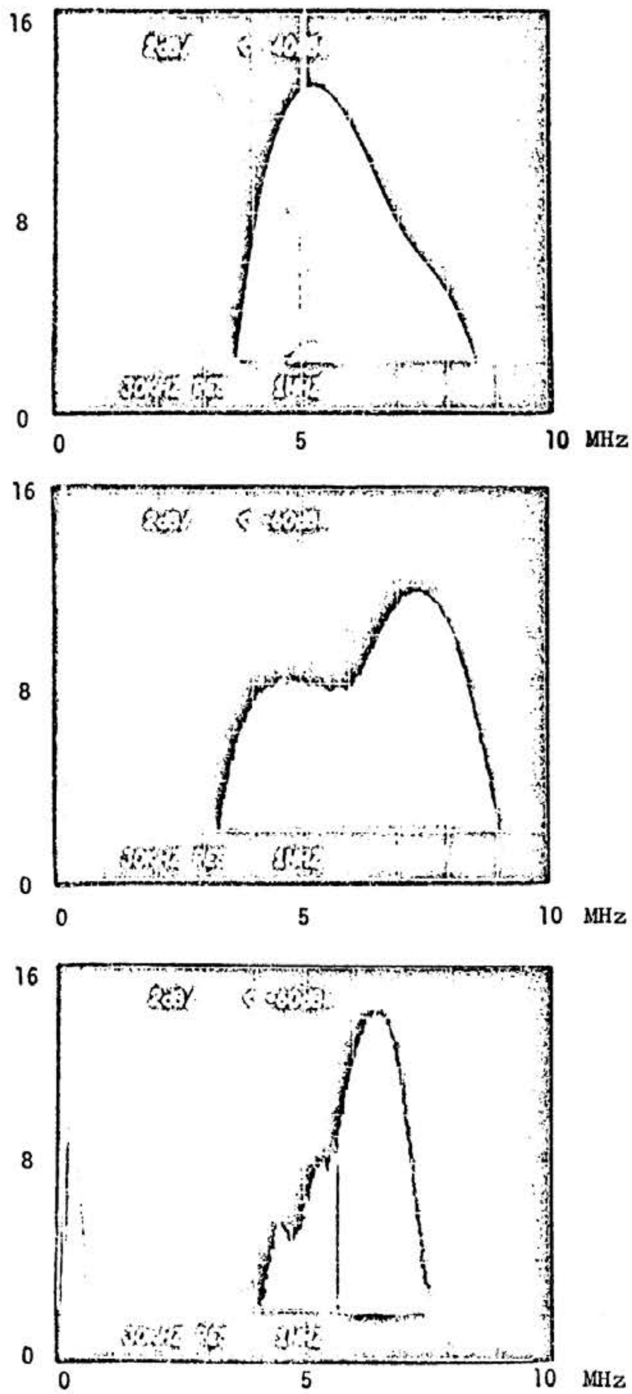


a. Spectrum of 0.5 Inch Diameter Transducer S/N 2848

b. Spectrum of 0.75 Inch Diameter Transducer S/N 2563

c. Spectrum of 1.0 Inch Diameter Transducer S/N 2663

Fig. 3. Spectra of three 5 MHz transducers used to collect data.

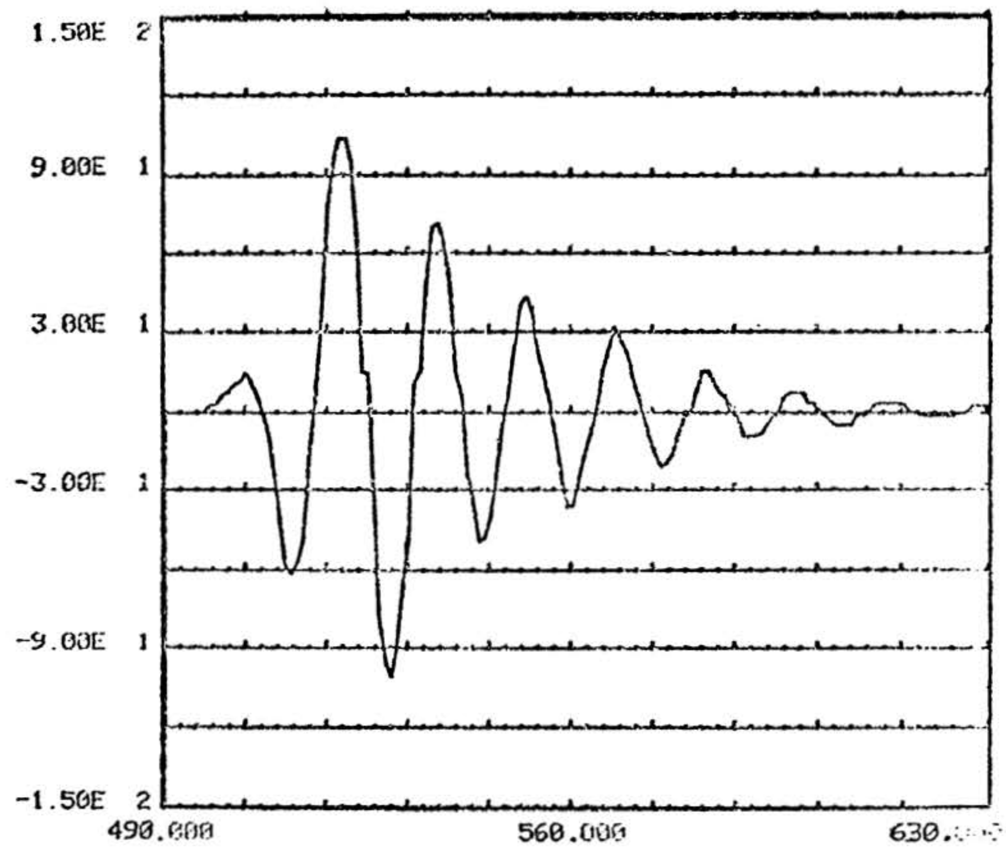


Fig. 4. Plot of significant test data from backwall echo of test number 127.

The distribution of the experimental data recorded among the four subsets is given in Table I. The uses of the fitting and selection subsets in the ALN classifier synthesis are described in detail in (3, 10, 11, 12, 13). The 49 tests employed in this project were those experiments (of the 127) that were echoes from the defect, not the backwall, and were not clipped or otherwise improperly recorded.

Each experimentally recorded pulse echo time waveform was corrected for three instrumentation settings: sensitivity (S), attenuation (B), and damping (D). The correction is multiplicative in the following form: $x'(t) = SBD\, x(t)$

Recorded waveforms can vary greatly for the same size hole due to different characteristics among various transducers and transmission media. An example of these differences, from our work, is shown in Fig. 5. Here, the maximum amplitude has been plotted for each of the eight defects, as recorded from three different 5 MHz transducers and two different sets of the 7075-T6 aluminum blocks. Each of the waveforms was corrected with respect to sensitivity, attenuation and damping according to the above Equation prior to reading the maximum amplitude. It can be seen that there is a monotonically increasing relationship between hole size and maximum amplitude within each of the five test series. In no case is this relationship violated. Consequently, one would be led to believe that maximum amplitude was a key defect size discriminator if only one of the above series were recorded.

It is evident from the figure that this conclusion is not valid for other transducers and media. The maximum amplitude shows significantly large variations between the five series. For instance, the maximum amplitude of a Number 5 hole using a 0.5 inch transducer on the RM/AI blocks (Fig. 5(a)) is very close to that of a Number 6 hole for the same material using a 0.75 inch transducer (Fig. 5(b)). Continuing across the figure, this value lies between those recorded for hole Numbers 7 and 8 for the same 0.5 inch transducer, but with the Trienco blocks (Fig. 5(c)). The Number 5 hole would be classified as a Number 8 hole using a 0.75 inch transducer with the Trienco blocks or using a 1 inch transducer with the RM/AI blocks (Fig.s 5(d)) and 5(e), respectively.)

Mistakes of three hole sizes could be made merely by changing transducers and/or test block media if one relied strictly on the maximum amplitude as a discriminating feature. These results dramatize the problem associated with solely using maximum amplitude.

One way of reducing the sensitivity to transducer/medium differences has been advanced by Frederick and Seydel[8]. According to these authors, a convenient way of viewing the recorded pulse echo UNDT signal is as shown in Fig. 6. It can be seen that the recorded signal is a function of four quantities: the pulser, the transducer, the medium, and the discontinuity itself. If, in fact, the actual recorded signal was produced by a convolution process, this figure would be accurate and the transfer function of the resultant signal in the time and frequency domain would be as shown at the bottom of the figure. It is known that this linear representation of the system response is not correct and that the process is nonlinear. However, the structure shown in Fig. 6 is a convenient way of viewing the

Table I. Distribution of the 49 Experimental Data Records Among the Four Data Subsets.

| Hole Size (in 64th's) | Data Subset: Fitting | Selection | Evaluation #1 | Evaluation #2 |
|---|---|---|---|---|
| 8 | 0.5"T, 0.75"R | 0.75"T, 0.75"R | 0.5"R, 0.75"R(2) | 1"R |
| 7 | 0.75"T, 0.75"R | 0.5"R, 0.75"R | 0.75"R(2) | 1"R |
| 6 | 0.5"R, 0.75"R | 0.5"T, 0.75"R | 0.75"T | 1"R |
| 5 | 0.5"T, 0.75"R | 0.75"R | 0.75"T, 0.5"R | 1"R |
| 4 | 0.75"T, 0.75"R | 0.5"R | 0.5"T, 0.75"R | 1"R |
| 3 | 0.75"T, 0.75"R | 0.5"T | None | 1"R |
| 2 | 0.5"T, 0.75"R | 0.75"T, 0.75"R | 0.5"R | 1"R |
| 1 | 0.75"T, 0.75"R | 0.5"T, 0.5"R | 0.75"R | 1"R |
| Total: | 16 | 13 | 12 | 8 |

T = Trienco test blocks

R = Reynolds Metal test blocks

0.5" = 0.5-inch Parametrics 5 MHz transducer

0.75" = 0.75-inch Parametrics 5 MHz transducer

1" = 1-inch Parametrics 5 MHz transducer

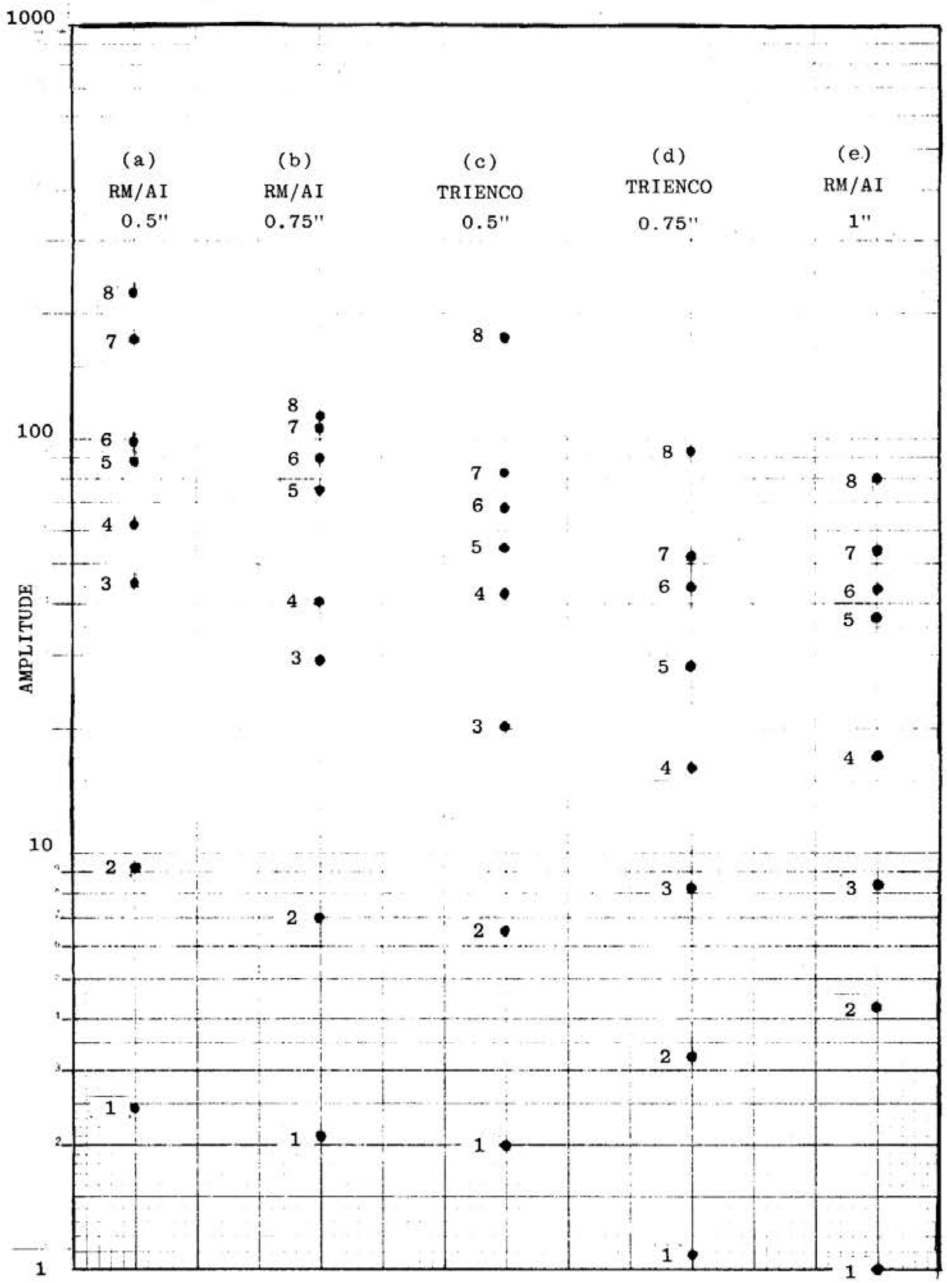


Fig. 5. Corrected maximum amplitude for 1/64" to 8/64" flat-bottom holes.

Three different 5 MHz transducers and two different test sets of 7075-T6 Aluminum area-amplitude blocks were used.

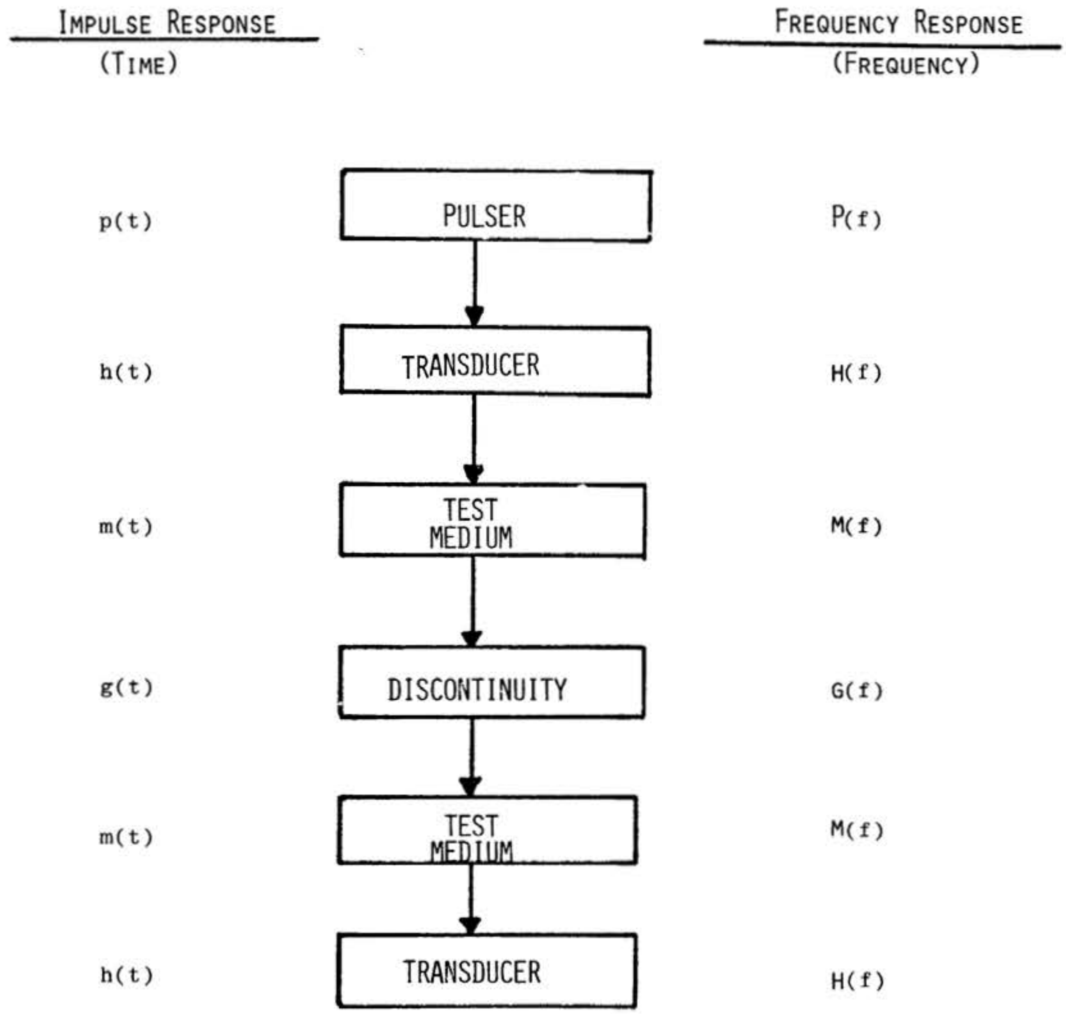


$f(t) \approx h(t)*m(t)*g(t)*m(t)*h(t)$ = UNDT OUTPUT

$F(f) \approx H^2(f)\ M^2(f)\ G(f)$

Fig. 6. Structure of a pulse echo ultrasonic nondestructive testing system.

physical phenomena and it provided guidance for appropriate ways to reprocess the data prior to waveform parameterization.

One of the key goals is to eliminate or at least reduce the sensitivity of the resultant classification system to variations due to different transducers and media as described above. One approach is to use the structure in Fig. 6 as a waveform preprocessing guide in the following way. If the recorded signal were truly a convolution of the respective pulser, transducer, medium, and discontinuity transfer functions, the transducer and medium effects could be removed by performing the inverse mathematical operation, namely deconvolution. This is accomplished by using a reference test signal whose transducer and test medium characteristics are the same as the unknown signal. The Fourier transform of both the reference signal, R(t), and the unknown test signal, U(t), is taken and R is deconvolved from U by dividing the two transformed signals, point-by-point, in the frequency domain. The inverse Fourier transform then converts the signal back to the time domain, presumably "stripped" of transducer and medium effects.

The deconvolution process induces artifactual high frequency content in the resultant waveform (6, 8, 14, 15, 17, 18). This is largely suppressed by a smoothing operation known as a "Hamming Window". A three-point triangular waveform normalized to unit area (values = 1/4, 1/2, 1/4) is convolved with the deconvolved signal prior to the inverse Fourier transform step. (The "Hamming Window" is a first-order approximation to a Gaussian distribution and, as such, induces no lead or lag effects in the smoothed waveform.) All of the above preprocessing steps are shown in Fig. 7.

At first, the reference waveform used for a given series of tests was the backwall echo obtained from the no-hole block. However, this reference waveform was found to be sensitive to medium but not to transducer variations. It was then decided to use one of the eight holes as the reference waveform. The Number 1 hole was arbitrarily chosen for this purpose.

Once the U"(f) signal was obtained (as shown in Fig. 7), a number of other waveforms could be generated from it. These include: (1) Time Waveform-via an inverse Fourier transform; (2) Power Spectrum - via the sum of the squared real and imaginary components; (3) Auto Correlation - via an inverse Fourier transform of the Power Spectrum; (4) Cepstrum - via a Fourier transform of the logarithm of the Power Spectrum; (4) Log Power Spectrum - via the logarithm of the frequency axis. The Cepstrum is useful for detecting periodicities in the Power Spectrum. The Log Power Spectrum greatly emphasises the low end of the frequency band. (The frequency band was 0 to 40 MHz in our work).

A set of parameters can be computed from this array of waveforms generated from the single pulse echo waveform for a single experiment. Amplitude is a popularly used feature and it does contain defect size discriminatory information -- at least for a given transducer and medium. It was decided to compute the square of the deconvolved waveform in order to greatly emphasize any large amplitudes in the signal. Therefore, after the deconvolution preprocessing step, the deconvolved time waveform, U"(t), and its square, $U''^2(t)$, were available for further processing.

Each of these signals was then subjected to the computations shown above; namely, the Power Spectrum, Auto Correlation and Cepstrum of each of the two

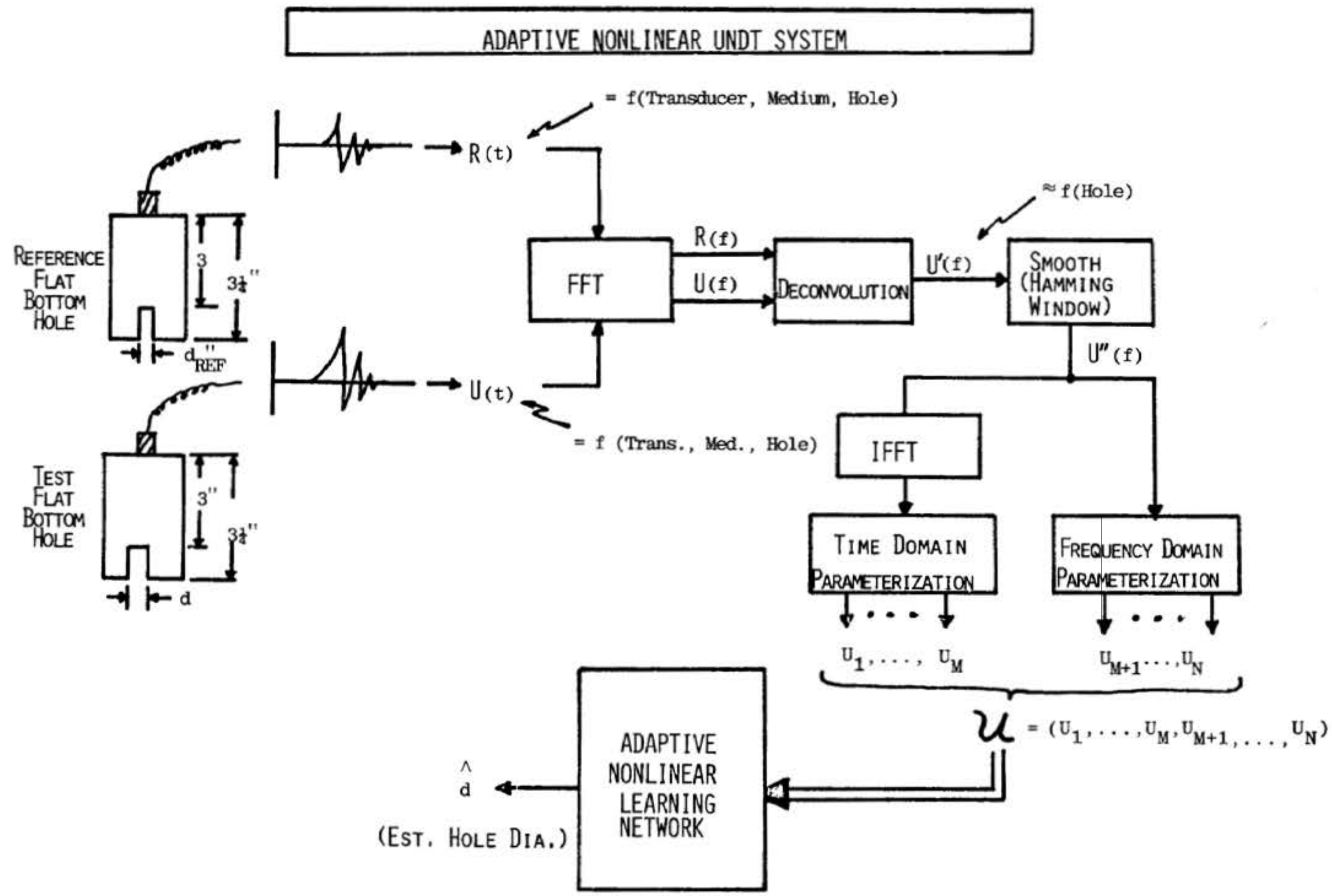


Fig. 7. Adaptive nonlinear UNDT system.

signals were generated. (The Log Power Spectrum was not used). There were now three waveforms computed from each of the two time waveforms, for a total of eight waveforms per experiment shot. Four types of parameters were computed from each of the eight waveforms: statistical, shape, area, and extremal.

The statistical parameters consist of four descriptors of the global properties of a waveform: mean, variance, maximum, and minimum.

The shape parameters are five global descriptors that account for the overall shape of a waveform. The first, $S_1$, is the area under the curve. The second, $S_2$, is a weighted area normalized by $S_1$. Parameter $S_2$ could, for example, identify two identically shaped waveforms offset by a DC bias. Parameter $S_1$, on the other hand, would be sensitive to the bias. Depending on whether or not the bias was a discriminating feature between two different defects, $S_1$ or $S_2$ would be appropriate. The other three S parameters measure properties of the waveform such as skewness and other forms of asymmetry. These parameters are analogous to skewness and Kurtosis in univariate statistics.

The area parameters are descriptors of local regions of a waveform. The waveform is divided into four equal and contiguous parts and $B_i$ is the area contained within the $i^{th}$ part. (Notice that $S_1$ is equal to the sum of the four B's).

The extremal parameters are local descriptors that are equal to the maximum value of the waveform within a particular data window. The windows are overlapping. So, if the waveform possessed only one maximum and decreased monotonically on either side of it, and if this maximum was located within the first window, all four W's would be equal. If this maximum shifted to the second window, $W_2$, $W_3$, $W_4$ would be equal and different from $W_1$. Thus, a moving peak would be detected. Also, a waveform with a number of local maxima would generally yield four different W's and this waveform could be discriminated from one with fewer local maxima.

The total number of (candidate) parameters computed was ninety-six and this parameter set contains both local and global descriptors of a particular waveform. The parameters are of a rather general nature and not specifically motivated by this flat-bottom hole classification problem. Therefore, it was felt that their successful employment in the ALN classifier model would further demonstrate the generalability and flexibility of this approach.

A rigorous capability exists for synthesizing nonlinear, multivariate models that can infer flaw geometry with very high accuracy. The result of this approach is called a nonlinear adaptive learning network (ALN). The methodology associated with ALN's is described in more detail in references (3, 10, 11, 12, 13) by Mucciardi and Barron.

An ALN was trained via the methods summarized in these references using the four data subsets and the parameters described above. Thus, the information used for each experiment was as follows: input variables--ninety six parameters of the record pulse echo; output variable --diameter of the flat-bottom hole. Characteristics of the transducer and medium were not used; indeed, the purpose of the waveform preprocessing and ALN synthesis steps was to remove these effects as much as possible.

The Fitting and Selection data subsets (Table I) were used to train the ALN classifier. In this training exercise, the output variable was used for model synthesis. After the ALN was obtained, the two evaluation subsets were input to the model to test its ability to infer hole sizes for experimental data not used in the design (i.e., training) phase. The output variable of the Evaluation subset data was not presented to the classifier. (Twenty-nine of the 49 available records were used for classifier design as shown in Table I).

The synthesized ALN is shown in Fig. 8. It can be seen that only 15 of the 96 parameters proved to be informative for discriminating the various hole sizes. The three-layered network implements a multinomial (A polynomial in many variables) up to degree eight in the 15 input variables.

A major result was that maximum amplitude was not among the 15-member informative subset. This substantiates findings shown in Fig. 5--that maximum amplitude is very sensitive to transducer and media differences and, hence, is not a highly discriminating parameter.

Among the most informative fifteen member parameter subset, the total energy in the lowest quarter of the frequency band, 0-12.5 MHz, was a key parameter. It was paired with three other parameters as shown in Fig. 8. It can be seen that the Power Spectrum and its Fourier transform--the Cepstrum--contain most of the information relative to hole size discrimination. In addition, the area contained under certain portions of these two waveforms and their overall shape bear significant defect size information. An informative Cepstrum implies periodicities in the Power Spectrum. These periodicities could in fact be due to inherent physical phenomena or they could be introduced by the deconvolution procedure. This latter explanation could also account for the appearance of an informative parameter in the highest portion, 37.5 to 40 MHz, of the Power Spectrum.

Another factor to bear in mind regarding the best found parameter subset is that the deconvolution procedure may remove some of the physical meaning from the resultant waveform. That is, the deconvolved signal is not a physical signal in the sense that it is not recorded by a transducer. Instead, it is generated inside the computer by transforming the recorded signal. It is known that periodicities are induced in the spectrum of the deconvolved signal by the deconvolution process. Hence, this may be one of the reasons why the Cepstrum is so important. This hypothesis could be tested by retraining the network using the same parameters, but eliminating the deconvolution preprocessing step. If a different subset of parameters was identified that yielded equivalent results, then the above conjecture would be true.

The hole sizes inferred by the network (Fig. 8) are listed in Table II. The inferences for the 16 tests in the Fitting data subset are circled. The inferences for the 13 tests in Selection data subset are denoted by broken circles. The remaining 20 uncircled numbers are the network inferences for

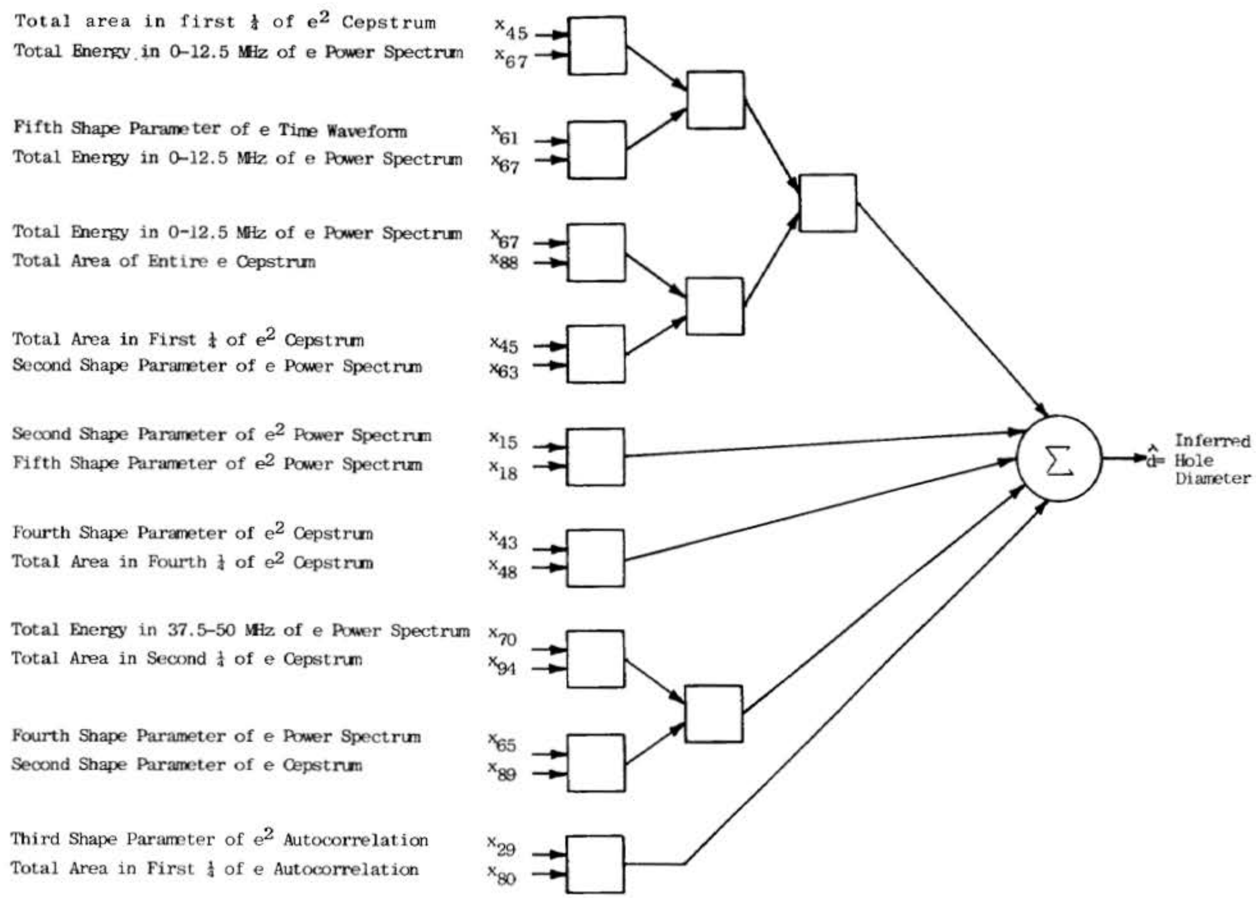


Fig. 8. ALN Flat-bottom hole classifier structure.
$e$ is the pulse echo time waveform
$e^2$ is the squared pulse echo time waveform

Table II. Predicted Diameter of Flat-bottomed Holes by the Use of Adaptive Training Networks

A solid circle denotes a fitting subset record; a broken circle denotes a selection subset record; remaining records are in both evaluation data subsets.

| Test Conditions / Hole Size (in 64th's) | Trienco Block 0.5" Transducer | Trienco Block 0.75" Transducer | Reynolds Metal 0.5" Transducer | Reynolds Metal 0.75" Transducer | | Reynolds Metal 1" Transducer |
|---|---|---|---|---|---|---|
| 8. | 8.0 (46) | 8.0 (25) | 8.2 (86) | 7.8 (107) 8.2 (74) | 7.9 (98) 7.8 (110) | 8.1 (119) |
| 7. | (48) | 6.8 (27) | 7.0 (87) | 7.0 (108) 7.2 (75) | 7.1 (99) 6.4 (109) | 6.7 (120) |
| 6. | 4.4 (50) | 6.1 (29) | 6.0 (88) | 6.1 (76) | 5.7 (100) | 6.0 (121) |
| 5. | 4.7 (52) | 4.8 (31) | 5.5 (89) | 5.1 (77) | 5.0 (101) | 5.2 (122) |
| 4. | 4.0 (54) | 4.3 (33) | 4.0 (90) | 4.2 (78) | 4.2 (102) | 4.0 (123) |
| 3. | 3.0 (58) | 3.0 (36) | | | 2.9 (103) | 2.2 (124) |
| 2. | 2.1 (60) | 2.0 (38) | 2.3 (92) | 1.9 (80) | 2.0 (105) | 2.4 (125) |
| 1. | 1.0 (62) | 1.0 (40) | 1.0 (93) | 1.0 (81) | 1.0 (106) | 1.0 (126) |

the data in both Evaluation data subsets. (Recall that Evaluation Subset 2, the last column in Table II, consisted exclusively of the 1 inch transducer series, and that none of these eight waveforms was included in either the Fitting or Selection subsets used to train the ALN classifier.

Only 3 misclassifications occurred out of 49 possibilities. The three errors were:

(1) Number 6 Trienco block hole called a 4 hole using a 0.5 inch transducer;

(2) Number 7 Reynolds Metal block hole called a 6 hole using a 0.75 inch transducer;

(3) Number 3 Reynolds Metal block hole called a 2 hole using a 1 inch transducer.

An entry in the experimental logbook reported an improper recording for test 50--the first error given. The logbook entry noted that the transducer had been inadvertently moved from its center position and that a lower level signal had been recorded. This coincides with the smaller value of 4.4 predicted for the Number 6 defect. The third error (on the Number 3 hole) may be due to the fact that data from this size defect are least represented in the experimental series. As a consequence, the network was least trained in recognizing this defect size.

Overall, it can be seen from Table II that the ALN flat-bottom hole classifier is extremely accurate. If the questionable error on the Number 6 hole is not counted, 46 out of 48 correct classifications were rendered (95.8%).

Another ALN was trained with the deconvolution step eliminated (Fig. 7). The accuracy rate (i.e., percentage of true defect size) decreased slightly with this model from 97.2 to 93.9 %. Therefore, the deconvolution step has been shown not to be critical in this case; the ALN can still cope well. Its effect is to slightly sharpen the accuracy rate. Based on the ALN classifier accuracy rate and its insensitivity to different transducers and media (three transducers and two sets of test blocks), it is concluded that this methodological approach has considerable utility in ultrasonic nondestructive evaluation.

Acknowledgments

The encouragement and guidance of Cecil Gwinn of the Air Force Avionics Laboratory is gratefully acknowledged. His support in the adaptive learning network approach is responsible in large part for theoretical advances and many successful applications. Steven Crist was instrumental in initiating this project. William Lawrie and Henry Reeves of Babcock & Wilcox recorded the ultrasonic data. This project is jointly sponsored by the Air Force Materials and Avionics Laboratories under Contract F33615-74-C-5122.

References

1. Adler, L. and H. L. Whaley, "Interference Effect in a Multi-Frequency Ultrasonic Pulse Echo and Its applications to Flaw Characterizations," J. Acous. Soc. Amer., 51, 3, March 1972, pp. 881-887.

2. Aldridge, E. E. and H. G. Tattersall, "Utilization of Ultrasonic Scatter," Proc. Ultrasonics '71 Conference pp. 49-51.

3. Barron, R. L., "Theory and Application of Cybernetic Systems: An Overview," Proc. IEEE 1974 National Aerospace Electronics Conference (NAECON '74), Dayton, Ohio, May 13-15, 1974, pp. 107-118.

4. Bergland, G. D. "A Guided Tour of the Fast Fourier Transform," IEEE Spectrum, 6, July 1969, pp. 41-52.

5. Blackman, R. B. and J. W. Tukey, The Measurement of Power Spectra, Dover Publications, 1959.

6. Bohme, J. F., "The Cepstrum as a Generalized Function", IEEE Trans. Information Theory, September 1974, pp. 650-653.

7. Fickler, S. I., Assessment of Ultrasonic NDT Interrogation, Nexon, Inc. Final Technical Report, under Contract F33615-73-C-5105, AFML/LLP, December 1973, AFML-TR-73-189.

8. Frederick, J. R. and J. A. Seydel, "Improved Discontinuity Detection Using Computer-Aided Ultrasonic Pulse-Echo Techniques," Welding Research Council Bulletin 185, June 1973, pp. 1-23.

9. Gilstrap, L. O., Jr., "Keys to Developing Machines with High-Level Artificial Intelligence," Proc. ASME Design Engineering Conference, New York, New York, April 19-22, 1971.

10. Mucciardi, A. N. and E. E. Gose, "An Automatic Clustering Algorithm and Its Properties in High-Dimensional Spaces," IEEE Trans. on Systems, Man, and Cybernetics, Vol. SMC-2, No. 2, April 1972, pp. 247-254.

11. Mucciardi, A. N., "Elements of Learning Control Systems With Applications to Industrial Processes," Proc. 1972 IEEE Conference on Decision and Control, New Orleans, La. December 13-15, 1972, pp. 320-325.

12. Mucciardi, A. N., "New Developments in Water Shed Pollution Forecasting Using Adaptive Trainable Networks, "Proc. 1974 IEEE Conference on Decision and Control, Dallas, Texas, October 2-4, 1974.

13. Mucciardi, A. N., "Adaptive Nonlinear Modeling for Ultrasonic Signal Processing," Proc. Interdisciplinary Workshop for Quantitative Flaw Definition, June 1974, D. O. Thompson, (ed.) AFML-TR-74-238, pp. 194-212.

14. Oppenheim, A. V. R. W. Schafer and T. G. Stockham, "Nonlinear Filtering of Multiplied and Convolved Signals," Proc. IEEE, 56, 8, August 1968, pp. 1264-1291.

15. Ramirez, R. W. "The Fast Fourier Transform's Errors are Predictable, therefore Manageable," Electronics, June 13, 1974, pp. 96-102.

16. Reswick, J. B., "Determine System Dynamics --Without Upset," Control Engineering, June 1955, pp. 50-57.

17. Rice, R. B. "Inverse Convolution Filters," Geophysics, 27, 1962, pp. 4-18.

18. Robinson, E. A., "Predictive Decomposition of Seismic Traces," Geophysics, 22, 4, October 1957, pp. 767-778.

19. Skolnik, M. I., Introduction to Radar Systems, McGraw-Hill, 1962.

20. Thompson, D. O. (ed.), Proc. of Interdisciplinary Workshop on Nondestructive Testing--Materials Characterization, November 13-15, 1972, AFML-TR-73-69, April 1973.

## DISCUSSION

DR. STEVE CRIST: Question in the back?

DR. SY FRIEDMAN (NSRDC): Essentially would you say that your method requires that you first select a range of transducer and test blocks that would, more or less, run the gamut of what you would expect your universal discourse to be or universal interest? If you happen to just fortuitously select a lot of transducers that are pretty much alike and materials that are pretty much alike, then this process really wouldn't tell you very much.

DR. MUCCIARDI: Well, that's not so, because we thought that was the case, but as you saw, we used three transducers here with very different characteristics, two of which were actually used in the synthesis procedures, and one that was not. In fact, it coped as well with the third as with the first two.

DR. FRIEDMAN: Well, the point is that they weren't--it was important here. Suppose the transducers were alike. You wouldn't really get any more information--

DR. MUCCIARDI: That is correct.

DR. FRIEDMAN: --out of two than you would out of one. That's what I'm driving at. So, if you have to take the trouble to have both the transducers and your materials vary somewhat.

DR. MUCCIARDI: Right. But it's not much trouble.

DR. FRIEDMAN: Well, I guess not. Secondly, these parameters, the 96 in all, what assurance do you have that they are truly independent?

DR. MUCCIARDI: Well, you have no assurance, and in fact, they're not independent. Our approach is to be somewhat exhaustive in the original parameter candidate list. Let's incorporate everything we can think of on intuitive and physical grounds and then let's sort through these. Those which, in fact, are redundant and those which are irrelevant will be sorted out by the procedures I have just described. This methodology can't recreate information, but it can sift through that which is available.

PROF. VERNON NEWHOUSE (Purdue University): I was at first very surprised when throughout today you have been saying that deconvolution didn't prove things; but on second thought I expect that what your computer system taught itself is probably what humans have taught themselves to some extent earlier, which was to do an envelope detection process on the signal and just look at the envelope. If that is true, in other words, if the examination criteria you used tend to confirm my guess, that they must be closely related to an envelope detection process--and remember, of course, for different frequency transducers, etc., you always tend to get the same envelope from the same kind of target. If that is true, then deconvolution would still help the computer in cases where you have two targets which are very close together, closer together than the transducer can resolve. So, you might find that when you get to the point of trying to analyze whether you have two targets present or three, then, deconvolution might still be very helpful.

DR. MUCCIARDI: Yes. I didn't, and I hope I didn't leave the intention that we were saying it's not useful at all. Our intent was to see what the process itself could do without this preprocessing step. In the case of other systems, it may be extremely useful. It can't hurt in this case; what it has done is to sharpen the results.

DR. CRIST: One more quick one?

MR. HARRY BERGER (National Bureau of Standards): Were there any surprises from a physics standpoint as to the 15 parameters that turned out to be useful, either in what was included or omitted in that list of 15?

DR. MUCCIARDI: Unfortunately, we haven't had the interaction with physicists that I wish we could. In fact, this is one of the reasons for being here and presenting these results and hoping to get some discussion started. From a physical point of view, one of the surprises was that amplitude or anything akin to amplitude, did not appear in the final model even in conjunction with other parameters.